ARCHIVES OF ELECTRICAL ENGINEERING VOL. 66(3), pp. 523-531 (2017)

DOI 10.1515/aee-2017-0039

Influence of the core saturation on the dynamic performance of the magnetostrictive actuator

KRZYSZTOF KOWALSKI, LECH NOWAK, ŁUKASZ KNYPIŃSKI, PAWEŁ IDZIAK

Institute of Electrical Engineering and Electronics, Poznań University of Technology
Piotrowo 3a, 60-965 Poznań
email: lukasz.knypinski@put.poznan.pl

(Received: 04.10.2016, revised: 16.02.2017)

Abstract: The paper considers the influence of core saturation on the dynamics of magnetostrictive fast-acting actuator. The field-circuit mathematical model of the dynamic operation of the capacitor-actuator system is applied. Two kinds of magnetostrictive core nonlinearity are taken into account. It has been proved that the saturation of the *B-H* curve practically does not affect the current, and capacitor voltage waveforms, but significantly affects a core elongation waveform. The computed results are compared with experimental ones.

Key words: magnetostriction, fast-acting actuator, finite element analysis, transient analysis

1. Introduction

In the case of limited linear motion actuators, the fast dynamic operations, i.e. short response time is very often required [6, 9]. In the most commonly used electromagnetic actuators the response time is of the order of millisecond up to hundred milliseconds [7, 9]. Therefore, the new structures in which force is generated by exploitation of other phenomena than those resulting from the interaction between a magnetic field and ferromagnetic elements are proposed [2, 12]. The paper deals with a system designed for the so called "high intensity plasma pulses gun" which is applied in the area of plasma physics and material engineering [1]. The magnetostrictive actuator is used as a driving device for a plasma gun valve. The device is supplied with capacitor discharge pulses. It is characterized by a very short response time – below 0.1 ms, but a relatively small displacement – less than 0.1 mm.

The magnetostriction effect is defined by the coefficient of the relative elongation $\lambda = \Delta l/l$. The unit of λ is expressed in micrometers per meter (μm/m) and is denoted by symbol ppm. Modern magnetostrictive devices are made of materials of the so-called giant magnetostriction (GMM) [5, 12]. The values of λ for these materials exceed 1000 ppm.

2. The device structure

The device has been designed to drive valve supplying fluid (usually gas) into the chamber of a pulse plasma gun, used for research in solid state physics, plasma physics and materials science [1]. A structure with an axisymmetric actuator has been proposed in Fig. 1 [3, 9].

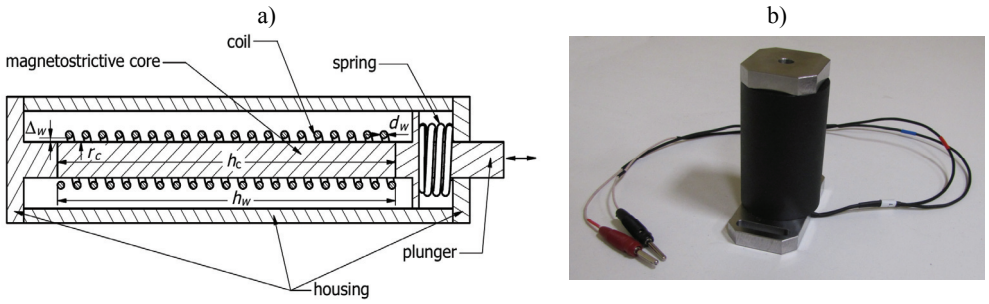

Fig. 1. Magnetostrictive axisymmetric actuator (a) structure, (b) prototype

The device is supplied with capacitor discharge pulses. During the charging the capacitors are connected in parallel in the battery, while during discharging they are connected in series. This allows to obtain a high initial discharging voltage.

There are two kinds of the nonlinearity of the system. The nonlinearity arises from: (a) nonlinear *B*-*H* curve and (b) nonlinear function $\lambda(H)$, see Fig. 2.

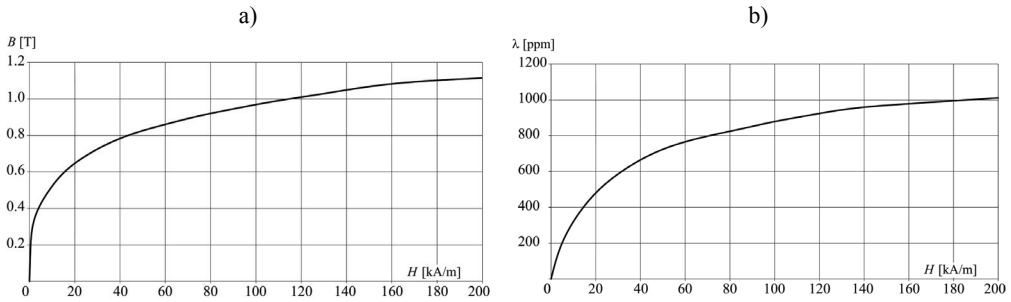

Fig. 2. Characteristics of the TERFENOL GMM material: (a) $B = f(H)$ and (b) $\lambda = f(H)$

In both cases a strong saturation effect can be observed. Both kinds of nonlinearity have to be taken into account.

3. Field-circuit model of transients of capacitor-actuator system

A structure with an axial symmetry has been proposed. The active magnetostrictive cylindrical element of the actuator is made of a GMM material and is placed within the solenoid. In

order to avoid the eddy currents, all parts of the device should be made of a material with a very high resistivity.

The magnetic circuit of the actuator contains non-linear parts. During the capacitors discharging, the electromagnetic field in the actuator is voltage-excited, and this means that the capacitor voltage $u_c(t)$ and winding current $i(t)$ are not known in advance [4, 9, 10, 11]. Therefore the field-circuit model of electromagnetic phenomena had to be applied. The field equations are coupled to the equation of the electrical circuit composed of R, C lumped parameters [11].

The magnetic field is described in cylindrical coordinate system r, z, φ. The mathematical model of electromagnetic phenomena consists of:

– The equation of the transient axisymmetric electromagnetic field in a non-linear medium

$$\vec{\nabla}\cdot\left(\frac{\nu}{\rho}\vec{\nabla}\Phi\right)=-J+\frac{\sigma}{\rho}\frac{\partial\Phi}{\partial t}. \tag{1}$$

– The equation of an electric circuit,

$$\frac{\mathrm{d}\Psi}{\mathrm{d}t}+Ri=u_c,\qquad \frac{\mathrm{d}u_c}{\mathrm{d}t}=-\frac{1}{C}i, \tag{2}$$

where: $\rho = 2\pi r$; $\Phi(r, z, t) = \rho A_\varphi(r, z, t)$; J is the current density; ν, σ are the reluctivity and conductivity of the considered regions, respectively; i, Ψ, are the current and winding flux linkage; u_c is the capacitor voltage; R is the winding resistance; C is the capacitance.

It has been assumed that the magnetic circuit of the device is made of nonconductive materials. The winding is made of thin wires (litz wire) and the spring is a polyester roller. The second term in the right-hand side of Equation (1) has been neglected.

The numerical implementation is based on the FE method and „step by step", Crack-Nicholson scheme [9]. At the n-th time-step, system of FEM equations can be written as

$$\boldsymbol{S}\boldsymbol{\Phi}_n=\mathbf{N}i_n, \tag{3}$$

where: $\boldsymbol{S}$ is the FEM stiffness matrix; $\boldsymbol{\Phi}_n$ is the vector of nodal potentials; $\boldsymbol{N}$ is the vector of "nodal turn numbers" [8, 11]. Because the field is voltage-excited the current value i_n in (3) is not know in advance. The circuit equation must be included. According to the Cranck-Nicholson scheme the discrete voltage equation takes the following form:

$$(0.5\Delta t)^{-1}\boldsymbol{N}^{\mathrm{T}}\boldsymbol{\Phi}_n+Zi_n=V_{n-1}, \tag{4}$$

where:

$$Z=R+0.5\Delta t/C,\quad V_{n-1}=u_{cn-1}+(0.5\Delta t)^{-1}\boldsymbol{N}^{\mathrm{T}}\boldsymbol{\Phi}_{n-1}+0.5\Delta t\left.\frac{\mathrm{d}u_c}{\mathrm{d}t}\right|_{n-1}+\boldsymbol{N}^{\mathrm{T}}\left.\frac{\mathrm{d}\boldsymbol{\Phi}}{\mathrm{d}t}\right|_{n-1}.$$

Because of the nonlinearity of the ferromagnetic core, the stiffness matrix $\boldsymbol{S}$ in (3) depends on the solution $\boldsymbol{\Phi}_n$ and i_n. Therefore it must be determined iteratively [3, 8]. In the proposed algorithm, the Newton-Raphson process has been adopted. In the k-th iteration, the vector $\boldsymbol{\Phi}_n$

in (3) and current i_n in (4) are replaced with increases $\delta\boldsymbol{\Phi}_n^k = \boldsymbol{\Phi}_n^k - \boldsymbol{\Phi}_n^{k-1}$ and $\delta i_n^k = i_n^k - i_n^{k-1}$. The vector $\delta\boldsymbol{\Phi}_n^k$ satisfies the set of equations

$$\boldsymbol{H}_n^k \cdot \delta\boldsymbol{\Phi}_n^k = \boldsymbol{R}_n^k, \tag{5}$$

where: $\boldsymbol{H}_n^k = \boldsymbol{H}\left(\boldsymbol{\Phi}_n^{k-1}\right)$ is the Jacobian matrix of the Newton-Raphson process [9, 10], $\boldsymbol{R}_n^k$ is the residual vector of equation (3), i.e.: $\boldsymbol{R}_n^k = \boldsymbol{N}\left(i_n^{k-1} + \delta i_n^k\right) - \boldsymbol{S}_n^k \boldsymbol{\Phi}_n^{k-1}$.

In the k-th iteration the current increase δi_n^k is not known in advance and therefore the vector $\boldsymbol{R}_n^k$ in (5) is not known either. Therefore, the field Equation (3) and circuit Equation (4) must be solved simultaneously. The following system of equations is obtained:

$$\begin{bmatrix} \boldsymbol{H}_n^k & -\boldsymbol{N} \\ \left(0.5\Delta t\right)^{-1}\boldsymbol{N}^{\mathrm{T}} & Z \end{bmatrix} \cdot \begin{bmatrix} \delta\boldsymbol{\Phi}_n^k \\ \delta i_n^k \end{bmatrix} = \begin{bmatrix} \boldsymbol{R}_{\Theta n}^{k-1} \\ \boldsymbol{R}_{Un}^{k-1} \end{bmatrix}. \tag{6}$$

The right-hand side of this system is explicitly known from the previous iteration and equal to:

$$\boldsymbol{R}_{\Theta n}^{k-1} = \boldsymbol{N} i_n^{k-1} - \boldsymbol{S}_n^k \boldsymbol{\Phi}_n^{k-1}, \quad \boldsymbol{R}_{Un}^{k-1} = V_{n-1} - Z i_n^{k-1} - \left(0.5\Delta t\right)^{-1} \boldsymbol{N}^{\mathrm{T}} \boldsymbol{\Phi}_n^{k-1}.$$

The computer software has been elaborated in Borland Delphi environment. The algorithm is very effective and stable. The studied actuator has been subdivided into 10080 triangular elements. The computation time for a single transient operations was approximately 2-8 second.

As a result of field-circuit computation the time-varying vector of nodal potentials $\boldsymbol{\Phi}(t)$ is obtained. Then the magnetic flux density, and magnetic field intensity are determined. The magnetostrictive core is divided by planes z = const into separate layers. On the basis of the characteristic $\lambda(H)$, the layers elongations are determined. The total elongation is computed as the sum of the elongations of separate layers.

The actuator with the cylindrical magnetostrictive core with a radius of r_c = 5 mm and a length of h_c =100 mm has been designed. Fig. 3 illustrates the absolute elongation Δh_m of separate core layers (m being the layer number) for five selected instants corresponding to winding ampere-turns equal to: (a) 16100; (b) 31000; (c) 44000; (d) 64300 and (e) 77000 A.

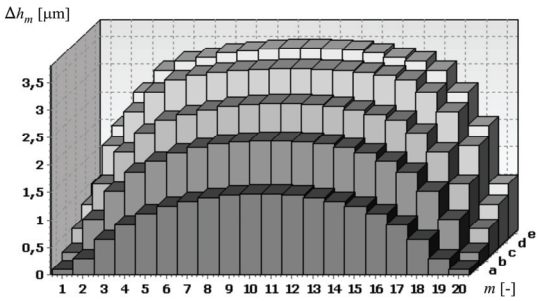

Fig. 3. Elongation of separate core layers

The non-homogenous distribution of magnetic field intensity and layers elongation along the core axis, as well the saturation effect can be observed. The field and elongation have the greatest values in the central part of the core. For greater current values the distribution becomes more uniform.

4. The influence of the magnetostrictive core saturation on the actuator dynamics

The actuator with the cylindrical magnetostrictive core with a radius of $r_c = 5$ mm, and a length of $h_c = 100$ mm and winding containing $N_t = 100$ turns made of thin wires has been designed. A total cross-section of 1.5 mm^2 for the conductor S_{cu} has been assumed. Because of the very short time of transients, the thermal effect is less important. A battery capacity (C) of 100 μF has been assumed. The transients, after the application of the capacitor voltage with an initial value of $U_0 = 460$ V have been considered.

In the design process of the device two main requirements have been assumed: (a) the response time $t_r \leq 0.05$ ms and (b) absolute elongation $\Delta h_r \geq 0.05$ mm.

The responses of the capacitor-actuator system, i.e. the winding current $i(t)$, capacitor voltage $u_c(t)$ and relative elongation $\lambda(t)$ are presented in Fig. 4.

a)

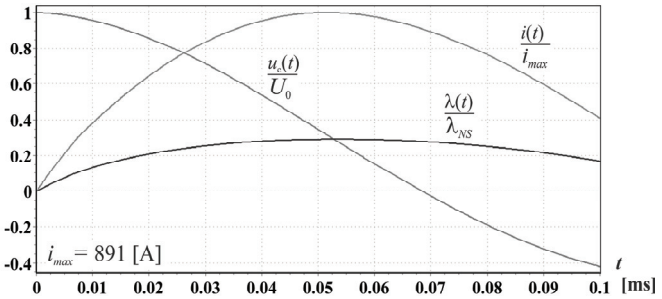

b)

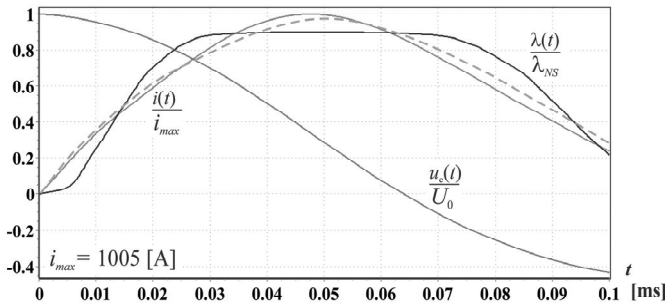

Fig. 4. The actuator transient response: a) for constant permeability $\mu_r = 110$, b) for non-linear B-H curve

In Fig. 4a, b, the current is related to the maximum value i_{max} of the first discharging current pulse, the capacitor voltage is related to its initial value U_0 and the elongation is related to the saturation value $\lambda_{NS} = 1100$ ppm of the catalogue characteristics $\lambda(H)$.

Two cases have been considered. In the first one, the linear *B-H* curve has been assumed – with a constant core relative permeability of $\mu_r = 110$. The actuator response in this case is shown in Fig. 4a. Fig. 4b illustrates the transient response of the actuator calculated on the basis of the real, non-linear *B-H* curve. In both cases the catalogue nonlinear elongation characteristic $\lambda(H)$ has been taken into account.

The dashed line in Fig. 4b illustrates the measured current *i*(*t*) in the winding of prototype actuator.

As it can be observed, the core saturation has a negligible effect on the electric quantities waveforms: capacitor voltage and winding current. This is because the reluctance of magnetostrictive core is very small in comparison to reluctance of the remaining part of the magnetic circuit, which is simply the air. The resultant inductance of the device practically does not depend on the core magnetic properties. Therefore, when electrical quantities are computed, the assumption of the linear *B-H* core characteristic is entirely acceptable.

Such assumption, however, is completely unacceptable in the case of the calculation of magnetic field intensity inside the magnetostrictive core and, as a result, it is also not acceptable in the calculation of the core elongation. Taking the saturation of the GMM material into account, the computed elongation is by almost 200 % greater than in the case of the simplified linear model.

For the precise nonlinear case (b) the maximum values $i_{max} = 1005$ A and $\lambda_{max} = 989$ ppm occurred at time $t_{max} = 0.051$ ms. However, practically, the maximum elongation (greater than 95% of λ_{max}) is achieved after a period of time of about 0.031 ms whereas a required value of 0.05 mm is reached very quickly – after $t = 0.0141$ ms, which is much shorter than a predetermined value of 0.05 ms. This means that obtained parameters meet the established design requirements.

In order to more thoroughly investigate the influence of GMM core saturation on the actuator dynamic operations, the simulations of a capacitor discharging process, assuming different values of the capacitor initial voltage U_0 has been performed. The voltage was being changed in the range from 50 to 950 V.

Figure 5 illustrates the influence of the voltage U_0 on the following parameters: (a) the maximal value of the first discharging current pulse i_{max}, (b) the maximal relative elongation λ_{max}, (c) time t_{max} after which the maximum point is achieved and (d) the time t_r after which a required elongation of 0.05 mm is reached. All parameters are related to the reference values: T_{REF}, I_{REF}, λ_{SAT}, where $T_{REF} = 0.054$ ms is the value of t_{max} obtained in the worst case, corresponding to the lowest voltage $U_0 = 50$ V, $I_{REF} = 2668$ A is the maximum pulse value of the current – corresponding to the maximum voltage $U_0 = 900$ V.

On the basis of the performed calculation it can be noticed, that the actuator achieved the optimal dynamic parameters for the saturation of $B(H)$ and $\lambda(H)$ characteristics corresponding to the initial voltage U_0 equal to approximately 400 V. For this voltage, the elongation reaches more than 95% of the maximum elongation λ_{SAT} of the GMM TERFENOL type ma-

terial. The increase of the voltage over 400 V has practically no effect on the core elongation increase. It only causes a slight decrease in the response time of the actuator.

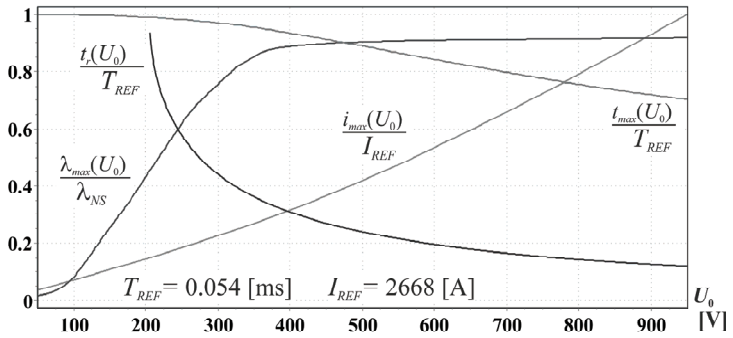

Fig. 5. Influence of the voltage U_0 on the actuator dynamics parameters $i_{\max}$, $\lambda_{\max}$, $t_{\max}$, t_r

It is obvious, that the degree of saturation depends not only on the voltage U_0. The value $U_0 = 400$ V is the optimal value only for the initially designed variant of the actuator with winding having $N_t = 100$ turns, supplied from the capacitor battery of the capacity $C = 100\ \mu$F. For another values of the capacity C the optimal degree of saturation occurs at another voltage U_0. The impact of capacity C on the parameters: $i_{\max}$, $\lambda_{\max}$, $t_{\max}$, and t_r is illustrated in Fig. 6. The parameters are related to the reference values: T_{REF}, I_{REF}, λ_{SAT}, where $T_{\mathrm{REF}} = 0.063\,\mathrm{ms}$, $I_{\mathrm{REF}} = 1157\,\mathrm{A}$ are the higher values of $t_{\max}$ and $i_{\max}$ – obtained for maximal capacitance $C = 200\ \mu$F.

The calculations have been performed for the previously determined optimum voltage $U_0 = 400$ V.

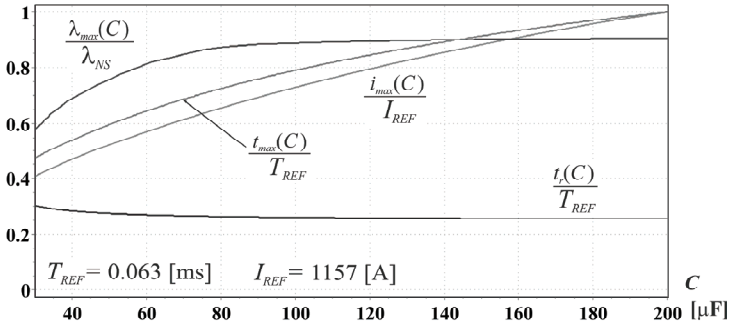

Fig. 6. Impact of the capacity C on the parameters $i_{\max}$, $\lambda_{\max}$, $t_{\max}$, t_r

The increase in capacity (as well as increasing the number of winding turns) clearly weakens the dynamics of the actuator and practically does not lead to an increase in elongation. This is because with an increase in capacity, the circuit resonant frequency decreases.

Thus the time period of vibrations and the time to reach the amplitude of the first capacitor current discharge pulse extends.

As it can be observed in Fig. 6, the maximum elongation is practically reached for the capacity $C = 80\ \mu$F. Increasing the capacity of more than this value does not have the effect of increasing the elongation λ_{max}.

The time t_{max} of reaching the maximum of the current pulse increases with the capacity increase. However, at the same time the amplitude of the first current pulse also increases, so that at the initial capacitor discharging stage, the slope of the waveform $i(t)$ is practically independent of the capacity C. Therefore, the time t_r until the required elongation $\Delta h_r = 0.05$ mm is reached, practically does not depend on the capacity value.

For the optimal selection of combinations of parameters, C, and U_0, the systematic, simultaneous review of their impact on the dynamics of the actuator should be carried out.

5. Conclusions

The elaborated algorithm and software could be a useful tool for the designing and optimization of the magnetostrictive, linear movement fast-acting actuators. The influence of the magnetostrictive core saturation on the dynamics of the actuator has been considered. The field-circuit mathematical model of the dynamic operation of the capacitor-actuator system has been applied. Two kinds of magnetostrictive core nonlinearity have been taken into account.

It has been proved that the assumption of linear B-H curve may leads to very large errors in determining the magnetostrictive sample elongation, even though it has little effect on the current and voltage waveforms.

In the future research, in order to find the best values of the capacity C and number N_t of winding turns, the optimization procedure will be included. The relative elongation λ_{max} and time t_r can be selected as the constraints of an optimization process.

References

[1] Barlak M., *Intense pulses of plasma processes to improve the wettability of the ceramic materials*, Publishing office Krystel (in Polish), Warsaw (2010).
[2] Engdahl G., *Handbook of giant magnetostrictive materials*, Academic Press, San Diego, USA (2000).
[3] Erping L., McEvan P.M., *Analysis of a circuit breaker solenoid actuator system using the coupled CAD-FE-Integral technique*, IEEE Transactions on Magnetics, vol. 28, no. 2, pp. 1279-1282 (1992).
[4] De Gersem H., Mertens R., Lahaye D., Vandewalle S., Hameyer K., *Solution strategies for transient, field-circuit coupled systems*, IEEE Transactions on Magnetics, vol. 36, no. 4, pp. 1531-1534 (2000).
[5] Evans P., Drapino M., *Dynamic model for 3-D magnetostrictive transducers*, IEEE Transactions on Magnetics, vol. 47, no 1, pp. 221-230 (2011).
[6] Harmer K., Jewell G.W., Howe D., *Transient performance of a short-stroke linear solenoid actuator*, IEE Proc. – Electric Power Appl., vol. 149, no. 5, pp. 379-384 (2002).

[7] Karunanidhia S., Singaperumal M., *Design, analysis and simulation of magnetostrictive actuator and its application to high dynamic servo valve*, Sensors and Actuators A: Physical, vol. 157, no 2, pp. 185-197 (2010).
[8] Knypiński Ł., Nowak L., *Field-circuit simulation of the dynamics of the outer rotor permanent magnet brushless DC motor*, COMPEL – The International Journal for Computation and Mathematics in Electrical and Electronic Engineering, vol. 30, no. 3, pp. 929-940 (2011).
[9] Nowak L., *Dynamic FE Analysis of Quasi-Axisymmetrical Electromechanical Converters*, IEEE Transactions on Magnetics, vol. 30, no. 5, pp. 3268-3271 (1994).
[10] Mikołajewicz J., Nowak L., *Reducing power loses in axisymmetric electromechanical converters*, COMPEL – The International Journal for Computation and Mathematics in Electrical and Electronic Engineering, vol. 25, no. 1, pp. 117-127 (2006).
[11] Piriou F., Razek A., *A Non-linear Coupled Field and Electric Circuit Equations*, IEEE Transactions on Magnetics, vol. 28, no 2, pp. 1295-1298 (1992).
[12] Stachowiak D., *Finite element analysis of the active element displacement in a giant magnetostrictive transducer*, COMPEL – The International Journal for Computation and Mathematics in Electrical and Electronic Engineering, vol. 35, no. 4, pp. 1371-1381 (2016).